EARTHQUAKE ENGINEERING AND STRUCTURAL DYNAMICS
Earthquake Engng. Struct. Dyn. **27**, 1541–1557 (1998)

IMPROVING EXPLICIT TIME INTEGRATION BY MODAL TRUNCATION TECHNIQUES

EUGENIO GUTIÉRREZ[1,*] AND JUAN JOSÉ LÓPEZ CELA[2]

[1]*Structural Mechanics Unit, Safety Technology Institute, Commission of the European Communities, Ispra 21020 (Va), Italy*
[2]*E.T.S Ingenieros Industriales, Universidad de Castilla-La Mancha, 13071 Ciudad Real, Spain*

SUMMARY

This paper describes a modal weighting technique that improves the stability characteristics of explicit time-integration schemes used in structural dynamics. The central difference method was chosen as the trial algorithm because of its simplicity, both in terms of formulation and ease of numerical stability and convergence analysis. It is shown how explicit algorithms may be reformulated in order to make them stable for any integration time by attenuating high-frequency oscillation modes that are generated by mesh geometry rather than generic dynamical features. We discuss results from trial calculations obtained from mathematical models that represent hysteretic restoring force elements and an application on a physical, four-degree-of-freedom, base-isolated structure using the pseudodynamic technique. © 1998 John Wiley & Sons, Ltd.

KEY WORDS: explicit algorithms; modal truncation; pseudodynamic tests; non-linear structural systems

1. INTRODUCTION

The great increase in electronic computing power over the past decades has resulted in the possibility of running finite element software that is capable of generating and solving equations related to very large and intricate structural models. Sometimes, the fine detail of those models is required in order to capture locally the effects of some generic loading. However, there is an inherent penalty in generating fine-detail systems, for the numerical approximations that are used to solve the related differential equations require discretizations in the independent variable that grows faster than the order of the mesh geometry.

In most structural engineering problems it is often required to study the effects of input forces whose time scale is much longer than that of the shortest structural period (the opposite is the case in impulsive or impact loads). For those cases it can be said that the structural response of a Multiple Degrees of Freedom (MDoF) non-linear system is made up of two oscillation mode sets. The first set, which contains the lower modes, is characterized by non-stationary eigenvalues and eigenvectors. The second set is made of higher modes whose eigenfunctions, generically, may also change but whose contribution to the global solution is negligible. In order to quantify their participation we could prescribe a modal norm that reflects their spectral contribution. Let us suppose we could segregate the high-mode set and then perturb it from some equilibrium point (this could arise as a result of some major structural non-linearity which affects primarily the low modes.) If we were to reexamine the high-mode set contribution about the new modal participation norm, we may find that it would not have altered the global response substantially.

The modal norm could aid us in deciding if an oscillation mode or set of modes is structurally important.

* Correspondence to: Eugenio Gutiérrez, European Commission, Joint Research Centre, Structural Mechanics Unit, TP 480, I-21020 Ispra (VA), Italy. E-mail: eugenio.gutierrez@jrc.it

CCC 0098–8847/98/121541–17$17·50

Received 29 July 1997
Revised 6 January 1998 and 9 April 1998

1.1. Analytical description of static condensation of high modes

First, we decompose the dynamical problem into uncoupled scalar equations via modal analysis: then we can examine each mode set in turn. We are interested in comparing the qualitative behaviour of the modes contained in a structural mode set.

Consider the Duhamel integral which expresses the linear response, of some intermediate nth mode as an infinite sequence of short impulses of length $\mathrm{d}\tau$, and for $t > \tau$. We can say that the modal structural response is given by:

$$x_n(t) = \int_0^t h(t-\tau)\, f_n(\tau)\, \mathrm{d}\tau \tag{1}$$

where $h(t-\tau) = \sin \omega_n(t-\tau)/m\omega_n$ is the unit response function and the system is at rest at its equilibrium position when $t = 0$. Now, if the modal forcing function is of the form $f_n(\tau) = F_n \mathrm{e}^{\mathrm{i}\omega_f \tau}$ and $1/\omega_f \gg t$, i.e. slowly varying in the interval of integration, the unit modal forcing function can be represented by a step function, in which case, the modal amplitude of the vibration is given by

$$x_n(t) = \frac{F_n}{m\omega_n} \int_0^t \sin \omega_n(t-\tau)\, \mathrm{d}\tau \Rightarrow x_n(t) = \frac{F_n}{m\omega_n^2}[1 - \cos \omega_n t] \tag{2}$$

where m is the orthonormalized modal mass which can be taken as unity.

The modal oscillation will thus be in the form given by Equation (2) and no dynamic amplification will take place. Hence, in a MDoF model, some of the higher modes will not be dynamically amplified if the expression $1/\omega_f \gg t$ is applicable. There is another consideration: we can compare the amplitude of the modal oscillations $F_n/m\omega_n^2$. Consider the ith and jth modes such that $\omega_j > \omega_i$. If we have that $F_j/m\omega_j^2 \ll F_i/m\omega_i^2$ and that the contribution of the ith is already small then, the contribution of the jth mode to the global response can be neglected. It is possible to use these criteria, or equivalent ones, to decide which modes are important or not depending on the magnitude of the modal amplitude. In this sense, what we have described above is only a diagnostic.

However, if we want to eliminate unwanted modes we require to define an algebraic operator in order to divide the original mode set into two modes: those we wish to retain and those we wish to eliminate. Thus, in this paper, we prescribe a method that truncates a modal basis from within the Cartesian basis during a numerical computation. The intention is to reform the structural problem so that it retains all the mesh detail whilst reducing the order of the spectral bandwidth in order to make the calculation less onerous than it would be for a full spectral content. However, the decision as to which modes are to be left out must be decided by the analyst.

1.2. About some relevant numerical integration algorithms

All explicit numerical time-integration procedures are conditionally stable. This is not a handicap when dealing with structural impact problems; one is constrained to use small time steps that are required by considerations of accuracy. In those cases, explicit schemes are generally more economical than implicit algorithms.

Implicit integration schemes may be made unconditionally stable. Some of them, such as the family of, so-called, HHT-method,[1,2] include tuneable numerical damping and are second-order accurate. However, the recursive implicit calculations, or matrix inversions during each time step can also become computationally expensive.

Another scheme is the, so-called, Operator Splitting method, developed by Hughes and Liu[3] and examined in Belytschko and Mullen,[4] which has been adapted to the pseudodynamic method.[5] These methods are semi-implicit in the sense that to implement them it is necessary to know the initial stiffness matrix of the

structure. In the event of structural non-linearities, the numerical stability is assured so long as the evolving eigenvalues are lower banded by the highest ones in the original linear case. The modal analysis approach is particularly useful in linear problems but it is not extensively used in non-linear ones; this is because the modal basis must be updated whenever the structural stiffness changes.

Non-linear modal techniques[6,7] can be adapted to use a truncated mode basis, but the solver must hop back and forth from modal to mesh co-ordinates. In these methods the modal co-ordinate serves as the kinematic basis, whereas the physical state parameters of the material are updated on the Cartesian co-ordinates. Some authors[8] report that, when using these techniques, numerical problems may arise from kinematic incompatibility whenever the modal basis is updated about an integration time step; if the update is performed too often chaotic oscillations may appear.

The method presented herein borrows heavily from the modal analysis techniques described above: it is a hybrid method that spans both the Cartesian and modal bases simultaneously. The numerical integration and the state variables of the structure are evaluated in Cartesian co-ordinates that describe the global solution. In step with that, a constant modal basis set (higher modes) is subtracted from that solution. In this sense there is no backward and forward motion from the Cartesian to the modal basis. However, by eliminating or detuning the highest oscillation modes, the permissible time step can be higher than what would otherwise be possible for the standard explicit scheme.

The criterion for defining the weighting functions is strictly related to the stability conditions that are consistent with the amplification matrix of that algorithm.

2. BACKGROUND DEFINITIONS

2.1. Equations of motion expressed in modal co-ordinates

The free vibration response of an undamped, elastic, second-order system is as follows:

$$\mathbf{M}\ddot{\mathbf{X}} + \mathbf{K}\mathbf{X} = \mathbf{0} \tag{3}$$

where, $\mathbf{M}$ and $\mathbf{K}$ are mass and stiffness matrices, respectively, of order n_{eq}. By introducing a change of basis to modal generalized co-ordinates[9,10] such a system may be expressed by n_{eq} uncoupled second-order equations. The following eigenvalue problems are formulated:

$$(\mathbf{K} - \lambda_l \mathbf{M})\boldsymbol{\Psi}_l = 0, \quad l \in \{1, 2, \ldots, n_{\text{eq}}\} \tag{4}$$

where

$$0 \leqslant \lambda_1 \leqslant \lambda_2 \leqslant \cdots \leqslant \lambda_{n_{\text{eq}}} \tag{5}$$

and

$$\boldsymbol{\Psi}^{\mathrm{T}}\mathbf{M}\boldsymbol{\Psi} = \mathbf{I} \quad \text{and} \quad \boldsymbol{\Psi}^{\mathrm{T}}\mathbf{K}\boldsymbol{\Psi} = \begin{pmatrix} \lambda_1 & & & \\ & \lambda_2 & & \\ & & \ddots & \\ & & & \lambda_{n_{\text{eq}}} \end{pmatrix} \tag{6}$$

The response of the system defined by equation (3) in terms of the modal co-ordinates is now

$$\mathbf{X}(t) = \sum_{m=1}^{n_{\text{eq}}} x_m(t)\boldsymbol{\Psi}_m \tag{7}$$

where x_m is the scalar modal expression of the mth mode shape, which is obtained from

$$x_m = \mathbf{\Psi}_m^{\mathrm{T}} \mathbf{M} \mathbf{X}(t) \tag{8}$$

Using equations (7) and (8) it can be shown that the following expression is the modal equivalent of equation (3):

$$\sum_{m=1}^{n_{\mathrm{eq}}} (\ddot{x}_m \mathbf{\Psi}_l^{\mathrm{T}} \mathbf{M} \mathbf{\Psi}_m + x_m \mathbf{\Psi}_l^{\mathrm{T}} \mathbf{K} \mathbf{\Psi}_m) = 0, \quad l \in \{1, 2, \ldots, n_{\mathrm{eq}}\} \tag{9}$$

Equation (9) can be simplified further by remembering the orthonormality properties. It follows that the independent lth modal equation is

$$\ddot{x}_l + \lambda_l x_l = 0 \tag{10}$$

Each of equations (10) may be solved numerically. The stability and accuracy of the global problem can be examined by observing the behaviour of the individual Single-Degree-Of-Freedom (SDoF) problems.

2.2. *Formulation of the modal problem in terms of central differences*

The solution of equation (3) may be expressed with the central difference recursive algorithm as follows:

$$\dot{\mathbf{X}}^n = \frac{\mathbf{X}^{n+1} - \mathbf{X}^{n-1}}{2(\Delta t)} \tag{11}$$

$$\mathbf{X}^{n+1} = (\Delta t)^2 \ddot{\mathbf{X}}^n + 2\mathbf{X}^n - \mathbf{X}^{n-1} \tag{12}$$

The acceleration term $\ddot{\mathbf{X}}^n$, which is the time-discretized form of the $\ddot{\mathbf{X}}(t_n)$, is found from equilibrium in equation (3).

In the linear elastic case, using equation (10) on the expression of type (12) for the lth mode we have

$$x_l^{n+1} = (2 - (\omega_l \Delta t)^2) x_l^n - x_l^{n-1} \tag{13}$$

where $\omega_l^2 = \lambda_l$ is the modal natural frequency squared.

Equation (3) can now be solved recursively by combining equations (8), (12) and (13) to give

$$\mathbf{X}^{n+1} = \sum_{m=1}^{n_{\mathrm{eq}}} [(2 - (\omega_m \Delta t)^2) x_m^n - x_m^{n-1}] \mathbf{\Psi}_m \tag{14}$$

The stability of this integration scheme is well documented[9,11] and is obtained by solving the eigenvalue problem of equation (10) for $l = n_q$, thus,

$$(\mathbf{A} - \omega^2 \mathbf{I}) = 0 \tag{15}$$

where $\mathbf{I}$ is the unit matrix and $\mathbf{A}$ is given by

$$\mathbf{A} = \begin{pmatrix} 2 - (\omega \Delta t)^2 & -1 \\ 1 & 0 \end{pmatrix} \tag{16}$$

and the modal suffix has been dropped. From equations (15) and (16) we have solutions of the form

$$\omega_{1,2}^2 = \bar{A} + \mathrm{i}\bar{B} \tag{17}$$

where

$$\bar{A} = 1 - \frac{(\omega \Delta t)^2}{2} \quad \text{and} \quad \bar{B} = \frac{\sqrt{4 - ((\omega \Delta t)^2 - 2)^2}}{2} \tag{18}$$

Stability criteria require that $(\bar{A}^2 + \bar{B}^2) \leqslant 1$ and that $\bar{B}$ is real. It can be shown that equation 13 is stable if $\omega\Delta t < 2$.

Also, the following terms are used to define the accuracy of the integration algorithm

$$\bar{\zeta} = -\frac{\ln(\bar{A}^2 + \bar{B}^2)}{2\bar{\Omega}} \tag{19}$$

$$\bar{\Omega} = \arctan\left(\frac{\bar{B}}{\bar{A}}\right) \tag{20}$$

The term $\bar{\zeta}$ is the numerical equivalent of viscous damping and $\bar{\Omega}$ is the effective sampling frequency.

In addition, the period distortion $T' = (\bar{T} - T)/T$ is defined as

$$T' = \frac{\omega\Delta t}{\bar{\Omega}} - 1 \tag{21}$$

For the central-difference algorithm we have $\bar{\zeta} = 0$ for all $\omega\Delta t$. It is important to note that the frequency distortion brings about a shortening of the period; hence, at the stability limit ($\omega\Delta t = 2$), even though the theoretical sampling frequency is π points per wave, in effect it is only two points per period, and consequently, unstable.

3. MODIFICATION TO THE CENTRAL DIFFERENCE ALGORITHM

3.1. For the single-mode case

A parameter, γ, is introduced which operates on $\omega\Delta t$. Equation (13) is modified as follows:

$$x^{n+1} = (2 - (\gamma\omega\Delta t)^2)x^n - x^{n-1} \tag{22}$$

where $1 > \gamma > 0$. If γ is confined to these values the effect is to increase the period of the vibration mode. It can be shown, through considerations of kinetic energy balance, that the period of oscillation is inversely proportional to γ.

In analogy to the standard central difference algorithm, the stability considerations are that $\gamma\omega\Delta t \leqslant 2$. Also, it can be shown that $\bar{\zeta}' = 0$ and that

$$\bar{\Omega}' = \arctan\frac{\sqrt{4 - ((\gamma\omega\Delta t)^2 - 2)^2}}{2 - (\gamma\omega\Delta t)^2} \tag{23}$$

Thus, the effective sampling frequency $\bar{\Omega}'$ can be tuned to lower frequencies in order to ensure numerical stability.

For every $\omega\Delta t$ there is a γ that makes the algorithm just stable: this value is referred to as $\gamma^0 = 2/\omega\Delta t$. In the limit, and remembering that $\arctan(-x) = \pi + \arctan(x)$, we reach $\bar{\Omega}' = \pi$. For $\omega\Delta t > \pi$ the minimum period distortion is given by the straight-line relationship:

$$T' = \frac{\omega\Delta t}{\pi} - 1 \tag{24}$$

3.2. Comparison of period distortion with trapezoidal rule

For the case of the modified central difference, and up to $\omega\Delta t < \pi$, the period error may be made arbitrarily close to zero by selecting a γ that minimizes the period error. After $\omega\Delta t > \pi$ we can use the value γ^0 as the weighting parameter, and the minimum period distortion is then given by equation (24).

The trapezoidal rule's effective sampling frequency is given by

$$\bar{\Omega}_{\mathrm{T}} = \arctan \sqrt{\left(1 - \frac{(\omega\Delta t)^2}{2(1 + 0.25(\omega\Delta t)^2)}\right)^{-2} - 1} \tag{25}$$

The value of $\bar{\Omega}_{\mathrm{T}}$ may be inserted into equation (21) to obtain the period error for the trapezoidal rule. Both the weighted central difference and the trapezoidal schemes shift all the frequencies to the left. This ensures that all vibration modes are represented by at least two integration points per wave. But, whereas in the trapezoidal rule this is performed automatically, in the weighted central difference formulation it is necessary to select the eigenvalues and eigenmodes we wish to keep.

If it were necessary to calculate the complete eigenvalue problem, this could become cumbersome for very large systems. Usually, the number of modes to be retained is low compared to the total, so, at the outset, it is only required to solve a reduced problem; the remaining dynamic modes can be omitted. The Cartesian representation, however, will be complete: in this sense the weighted algorithm is not a reduced system.

The trick is simple: unconditionally stable implicit schemes must shift the modal spectrum to the left and ensure a sampling period of two points per period. Alternately, the modes may be distorted, beforehand, to ensure stability in explicit numerical integration algorithms.

3.3. Formulation of modified central-difference for multi degrees of freedom

The stability and accuracy of the concepts described above may be extended to multiple-degree-of-freedom systems by way of standard modal analysis.

Using equation (22) for the modal basis defined in equation (7) results in

$$\mathbf{X}^{n+1} = \sum_{m=1}^{n_{\mathrm{eq}}} [(2 - (\gamma_m \omega_m \Delta t)^2) x_m^n - x_m^{n-1}] \boldsymbol{\Psi}_m \tag{26}$$

with some manipulation, and remembering that $-\omega_m^2 x_m^n = \ddot{x}_m^n$, the following expression is arrived at

$$\mathbf{X}^{n+1} = (\Delta t)^2 \sum_{m=1}^{n_{\mathrm{eq}}} \gamma_m^2 \ddot{x}_m \boldsymbol{\Psi}_m + 2\mathbf{X}^n - \mathbf{X}^{n-1} \tag{27}$$

To render the original formulation given in equation (12) stable for any Δt, it is sufficient to truncate the acceleration terms of the unstable modes by an amount given by

$$\gamma_u^2 = \frac{4}{(\omega\Delta t)_u^2} \qquad \{u | u \in \{1, 2, \ldots, n_{\mathrm{eq}}\}; (\omega\Delta t)_u \geqslant 2\} \tag{28}$$

Selective mode elimination is achieved by putting its corresponding $\gamma_l = 0$. This replaces the time-dependent dynamic mode as a pure stationary static mode; in this manner, only some modes are represented dynamically whilst others are only represented statically. Thus, for an n_{eq} degree of freedom system, the spectral representation will be one having $n_{\mathrm{s}} < n_{\mathrm{eq}}$ spectral co-ordinates. This is simply done by performing the summation in equation (27) up to n_{s}. However, as stated earlier, the number and disposition of Cartesian co-ordinates remains unaltered.

If, as expected, the retained modes change as a result of some structural non-linearity, the numerical stability is assured as long as the effective sampling frequencies (given by equations (23)) remain within the stability limits of the central difference algorithm.

Comparing equations (12) and (27), the only difference is the tuning (or exclusion) of the truncated terms. Equation (27) can be expressed in matrix form as

$$\mathbf{X}^{n+1} = (\Delta t)^2 \boldsymbol{\Psi} \boldsymbol{\Gamma} \boldsymbol{\Psi}^{\mathrm{T}} \mathbf{M} \ddot{\mathbf{X}}^{\mathrm{n}} + 2\mathbf{X}^{\mathrm{n}} - \mathbf{X}^{\mathrm{n-1}} \tag{29}$$

and

$$\mathbf{\Gamma} = \begin{pmatrix} \gamma_1^2 & & & \\ & \gamma_2^2 & & \\ & & . & \\ & & & \gamma_{n_{eq}}^2 \end{pmatrix} \tag{30}$$

In the limit case of mode elimination, the matrix expression for equation (27) is

$$\mathbf{X}^{n+1} = (\Delta t)^2 \overline{\mathbf{\Psi}}\, \overline{\mathbf{\Psi}}^{\mathrm{T}} \mathbf{M} \ddot{\mathbf{X}}^n + 2\mathbf{X}^n - \mathbf{X}^{n-1} \tag{31}$$

where

$$\bar{\mathbf{\Psi}} = [\mathbf{\Psi}_1 ... \mathbf{\Psi}_S ... \mathbf{\Psi}_{n_{eq}}] \tag{32}$$

In order to reduce the size of the eigenvalue problem only the modes up to $\bar{\mathbf{\Psi}}_S$ that are to be retained are evaluated. The remaining eigenvectors are not calculated but rather set to zero (with the advantage that the reduced eigenvalue problem may be orders of magnitude smaller than the complete one). This reformed eigenvalue matrix is kept constant for the duration of all the numerical calculation. Whereas the expressions in equations (29) and (31) are equivalent, it would seem more practical to use them in the form of equation (31) or the more primitive, but computationally cheaper form of equation (27). This is usually true of very large structural systems excited by low-frequency inputs.

3.4. Remark

It has been shown above, that the truncation is performed on the acceleration terms: it was chosen to demonstrate the stability characteristics of the amplification matrix. It was shown that the modal truncation may shift to the left the structural spectral content. This means that it is possible to choose a set of parameters that may shift the frequencies to the start of the spectrum. In the limit these modes may be tuned down to near-zero frequency, i.e. they reappear as drift. This distortion is remedied by performing the truncation directly on the displacement vector; this will attenuate any drift originating from the start-up conditions that may set off drift signals into motion.

4. RATE OF CONVERGENCE AND APPROXIMATION ERRORS

The numerical stability of the modified numerical scheme has been established. We can now examine the convergence rate (order of accuracy) by evaluating the local truncation error. The proof below is given for the SDoF expression, which also justifies the general multi-degree-of-freedom case via modal analysis. It will be shown that, for those modes that are not attenuated by the matrix $\mathbf{\Gamma}$, the rate of convergence is of order two. The proof,[10] is as follows:

For consistency, the time-discretized model of the homogeneous case may be written as

$$\mathbf{y}^{n+1} - \mathbf{A}\mathbf{y}^n = 0 \tag{33}$$

where

$$\mathbf{y}^{n+1} = \begin{pmatrix} x^{n+1} \\ x^n \end{pmatrix} \text{ and } \mathbf{A} = \begin{pmatrix} 2 - (\gamma\omega\Delta t)^2 & -1 \\ 1 & 0 \end{pmatrix} \tag{34}$$

To assess the error produced by iteration of the amplification matrix A, the term y^{n+1} is substituted for its exact value $\mathbf{y}(t_{n+1})$, where $t_{n+1} = (n+1)\Delta t$. Thus, the local truncation error is defined as

$$\mathbf{y}(t_{n+1}) - \mathbf{A}\mathbf{y}^n = \Delta t \tau \tag{35}$$

If we consider a simple solution, for example: free oscillations about some equilibrium given by

$$\mathbf{y}(t_{n+1}) = \begin{pmatrix} \cos((n+1)\omega\Delta t) \\ \cos(n\omega\Delta t) \end{pmatrix} \tag{36}$$

whereas the central difference approximation would be

$$\mathbf{A}\mathbf{y}^n = \begin{pmatrix} (2-(\gamma\omega\Delta t)^2)\cos(n\omega\Delta t) - \cos((n-1)\omega\Delta t) \\ \cos((n-1)\omega\Delta t) \end{pmatrix} \tag{37}$$

We can put $n = 1$ in expressions (36) and (37) and substitute in equation (35). Expressing all terms via Taylor expansion up to $O(\Delta t)^6$ and simplifying, we have

$$\tau = (\omega\Delta t)(\gamma^2 - 1) + (\omega\Delta t)^3(\tfrac{7}{12} - \tfrac{1}{2}\gamma^2) + O(\omega\Delta t)^5 \tag{38}$$

This equation states that residual first-order terms will cancel out if $\gamma = 1$, in which case the integration is second-order accurate. If $\gamma \neq 1$ the convergence rate will nominally be less than order two. Hence, the important modes will be treated up to second-order accuracy, whereas the truncated modes will not.

5. TRIALS

To demonstrate the performance of the integration scheme two examples have been chosen. The first one is a four-degree-of-freedom numerical system. The second one concerns an application to the pseudodynamic method using a full-scale, base isolated, moment-resisting steel frame.

To implement the reduction procedure we must first solve the initial eigenvalue problem. This need only be performed once for each structural model. The most usual case in seismic engineering is to consider the lower modes. Once the number of participating modes has been established, any number of calculations can be performed with the same participation factors given by equation (32). Only if the input motion were considerably changed in spectral content (i.e. if instead of an earthquake the input were a shock wave) would it be necessary to reappraise the vibration modes.

The problem could be posed as follows: we are carrying out a standard numerical integration that simultaneously subtracts the elastic modal participation of a set of higher modes representative of the system before any loading takes place. It is true that when the response becomes non-linear, the higher modes will change slightly, however, it will be shown that their participation is so small that this will not affect the accuracy of the major modes.

5.1. Example 1

We follow a similar example,[10] that consists of a system having a small number of degrees of freedom, but whose eigenvalues are widely spaced. The stiffness terms may become non-linear, in which case they follow phenomenological laws frequently used in seismic structural analysis[12] to represent reinforced concrete elements. No viscous damping terms have been considered and the masses are all unity. In order to introduce a wide variation in the eigenvalues, the stiffnesses have been selected using an analogy with simple beam theory as follows:

Consider a mechanical system that is represented in fine detail such as a bridge or a dam. The smallest element may be a 1000th of the total major dimension l say. The frequency of the oscillations increases with $1/l^2$, thus, a small discrete system will have the same spread of eigenvalues if the stiffnesses are chosen to grow with the power four. In the example given below the stiffnesses k_i are chosen so that $k_1{:}k_2{:}k_3{:}k_4$ as

$1{:}10^4{:}10^8{:}10^{12}$ which results in the following linear system matrices:

$$\mathbf{K} = \begin{pmatrix} k_1 + k_2 & -k_2 & 0 & 0 \\ -k_2 & k_2 + k_3 & -k_3 & 0 \\ 0 & -k_3 & k_3 + k_4 & -k_4 \\ 0 & 0 & -k_4 & k_4 \end{pmatrix}, \qquad \mathbf{M} = \begin{pmatrix} 1 & 0 & 0 & 0 \\ 0 & 1 & 0 & 0 \\ 0 & 0 & 1 & 0 \\ 0 & 0 & 0 & 1 \end{pmatrix}$$

$$\mathbf{\Psi} = \begin{pmatrix} 4{\cdot}9997\text{e}-01 & 8{\cdot}6604\text{e}-01 & -5{\cdot}4437\text{e}-05 & 1{\cdot}7678\text{e}-13 \\ 5{\cdot}0001\text{e}-01 & -2{\cdot}8861\text{e}-01 & 8{\cdot}1651\text{e}-01 & -3{\cdot}5357\text{e}-05 \\ 5{\cdot}0001\text{e}-01 & -2{\cdot}8861\text{e}-01 & -4{\cdot}0820\text{e}-01 & 7{\cdot}0712\text{e}-01 \\ 5{\cdot}0001\text{e}-01 & -2{\cdot}8861\text{e}-01 & -4{\cdot}0820\text{e}-01 & 7{\cdot}0712\text{e}-01 \end{pmatrix}$$

$$\omega = \begin{pmatrix} 4{\cdot}9995\text{e}-01 & 0 & 0 & 0 \\ 0 & 1{\cdot}1547\text{e}+02 & 0 & 0 \\ 0 & 0 & 1{\cdot}2238\text{e}+04 & 0 \\ 0 & 0 & 0 & 1{\cdot}4142\text{e}+06 \end{pmatrix}$$

The yield displacement is 1 m in all cases and the softening stiffness is $\frac{1}{10}$ of the original elastic one. The analogy with the beam-like structure simulates the onset of local plastic deformations as proportional to the local curvature of the beam in bending which, in the example given above, is consistent with the local (inter-mass) deformations.

It is interesting to compare the mode shapes of the elastic and non-linear cases. Consider a stage at which one of the stiffness elements has yielded so that $k_1 = 0.1k_1$ N/m; but, the remaining elements are unchanged. The post-yield eigenmodes and eigenvalues are

$$\mathbf{\Psi}_\text{d} = \begin{pmatrix} 5{\cdot}0000\text{e}-01 & 8{\cdot}6603\text{e}-01 & 5{\cdot}4437\text{e}-05 & 1{\cdot}7678\text{e}-13 \\ 5{\cdot}0000\text{e}-01 & -2{\cdot}8862\text{e}-01 & -8{\cdot}1651\text{e}-01 & -3{\cdot}5357\text{e}-05 \\ 5{\cdot}0000\text{e}-01 & -2{\cdot}8870\text{e}-01 & 4{\cdot}0820\text{e}-01 & 7{\cdot}0712\text{e}-01 \\ 5{\cdot}0000\text{e}-01 & -2{\cdot}8870\text{e}-01 & 4{\cdot}0826\text{e}-01 & 7{\cdot}0709\text{e}-01 \end{pmatrix}$$

$$\omega_\text{d} = \begin{pmatrix} 1{\cdot}5897\text{e}-01 & 0 & 0 & 0 \\ 0 & 1{\cdot}1547\text{e}+02 & 0 & 0 \\ 0 & 0 & 1{\cdot}2248\text{e}+04 & 0 \\ 0 & 0 & 0 & 1{\cdot}4142\text{e}+06 \end{pmatrix}$$

Comparing, respectively, eigenvalues obtained from the elastic and post-yield matrices it can be seen that only the lowest eigenvalue has been affected whereas the highest is not affected at all.

Now, we present some numerical trials. The following examples were obtained by subjecting the system to a forcing function given by:

$$\mathbf{F} = \omega_\text{f}^2 \cos(\omega_\text{f} t) * \mathbf{M} * \begin{pmatrix} 1 \\ 1 \\ 1 \\ 1 \end{pmatrix} \tag{39}$$

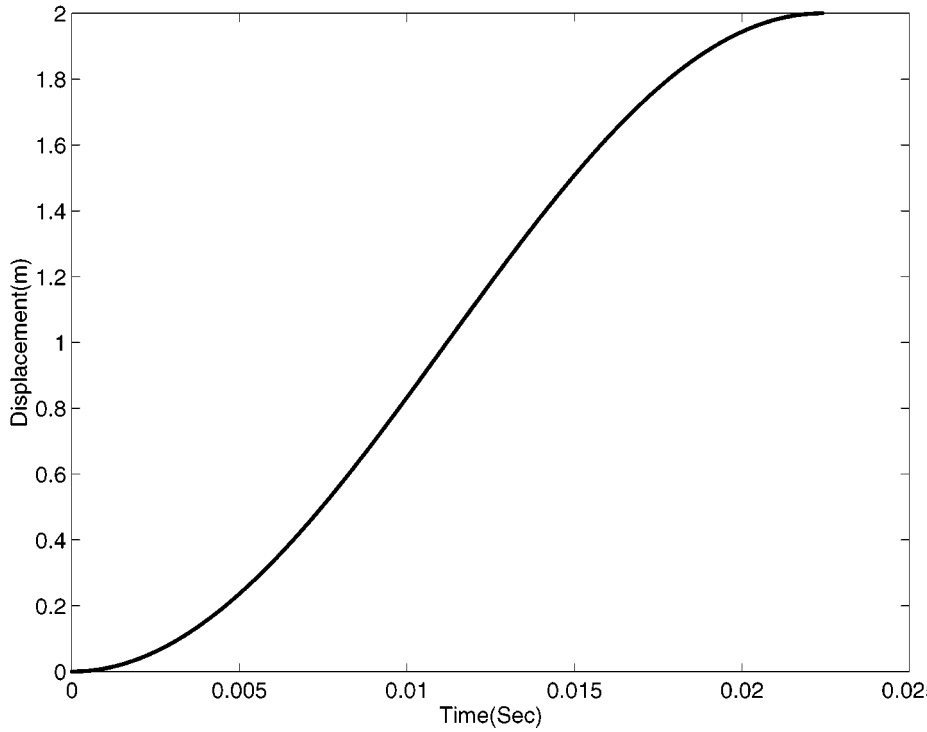

Figure 1. Displacement versus time signals of standard (continuous) and truncated (dots) methods for case 1

In case 1 $\omega_f = 140$ rad/s. This value is somewhat higher than the second mode in the discrete structure, but would be representative of a higher, interspersed, mode in a continuous beam-like structure. The standard central difference used a time step of 1·4e − 06 s, whereas the truncated solver used a time step of 1·4e − 04 s.

To model this system, under such a forcing function, it would be sufficient to consider only the first three modes and eliminate the fourth; a time-step larger by two orders of magnitude may now be used. Setting the matrix $\mathbf{\Gamma}$ in equation (29) as

$$\mathbf{\Gamma} = \text{diag}(1, 1, 1, 0) \tag{40}$$

while using the original mode matrix $\mathbf{\Psi}$, provided the following results. In Figure 1 we show the displacement of the first mass versus time for both the truncated and standard schemes; respectively, discontinuous and continuous lines that are indistinguishable. Even though the forcing frequency is quite high, the response of the system is well represented by a truncated mode basis. The response is not linear due to yielding in the spring at a displacement of 1 m.

Case 2 corresponds to a forcing frequency of 7 rad/s. The standard central difference algorithm was not used due to the excessive number of computational points needed to capture such a slow-varying signal. It was decided to compare the performance of the truncated formulation with an unconditionally stable implicit algorithm using the same time step as the truncated explicit form. Figure 2 shows the displacement signals whereas Figure 3 shows the force–displacement loops obtained for truncated and implicit schemes (discontinuous and continuous lines, respectively).

The fourth mode is so insignificant that, in all cases, the truncated and standard solutions overlap. It would be nonsensical to keep the fourth mode in the case of a system represented by so few elements. However, here it represents a set of high modes arising from the generation of fine mesh detail.

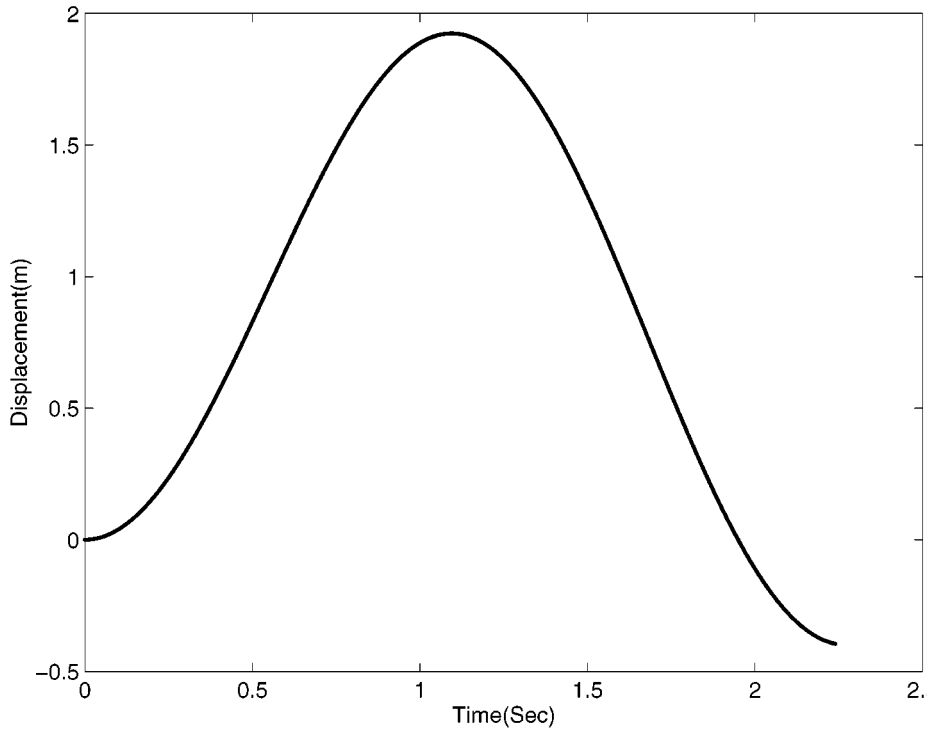

Figure 2. Displacement versus time signals of standard (continuous) and truncated (point–dash) methods for case 2

5.2. *Example 2*

In this example, the proposed method is tried out on a physical structure tested using the pseudodynamic method. The specimen, consisting of a three-storey, moment resisting frame was mounted on a set of rubber bearings which are used as seismic isolation devices.[13] The structure may be considered as a four-degree-of-freedom system. The kinematic degrees of freedom coincide with the three storeys that make up the building plus the base of the structure at the isolator anchoring stages. The actuators that drive the structure through the pseudodynamic test are mounted at the rubber base and at each storey. For the pseudodynamic method it is essential to use a numerical solver that arrives at the next displacement step monotonically in time. In view of this, care must be taken when using, so-called, implicit integration algorithms. The reason is that the structural response of a real structure undergoing inelastic deformations is conditioned by the path dependency. The pistons must drive the structure to the new target displacement monotonically. If the new displacement field was arrived at via non-monotonic trial increments that overshoot the eventual target field, the structural characteristics would be irreversibly affected by the real trial displacements generated by the implicit solver. The consequence of this would be that the new structural state matrix would be inconsistent with the virtual-displacement increment of that time step. Of course, none of these arguments apply to a pure numerical model where implicit schemes perform well. However, some semi-implicit schemes[5,14] have been developed for the pseudodynamic method, yet they retain the essential detail of arriving at the implicit solutions monotonically within the time interval.

Although in this experimental example the eigenvalues are not excessively dispersed, and the standard central difference scheme is more than adequate, it is instructive to perform trials of the truncation scheme on the pseudodynamic method.

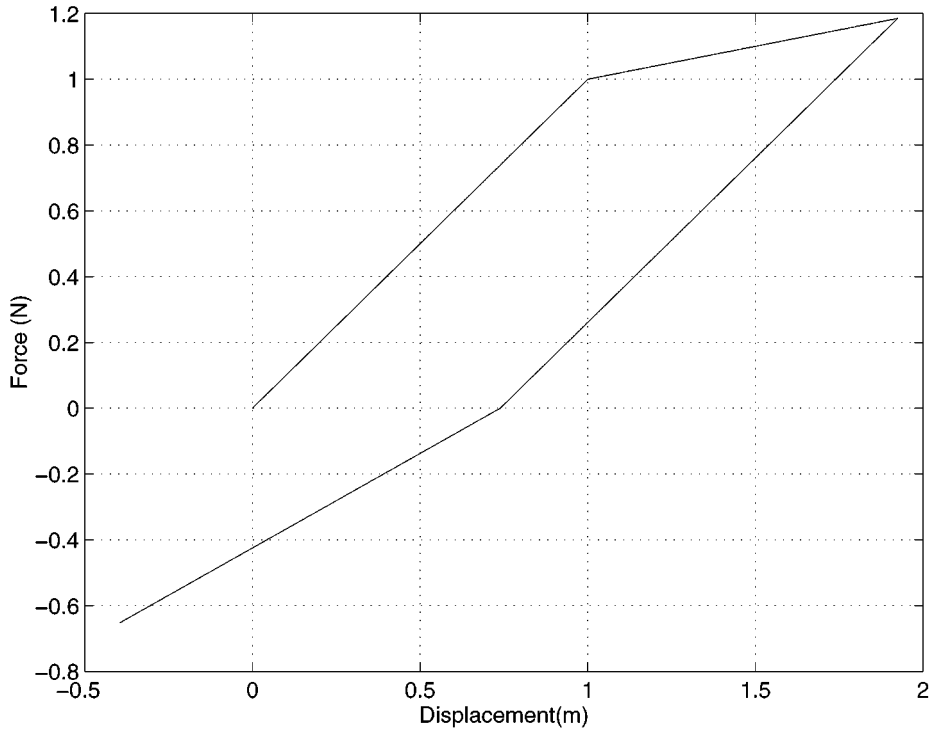

Figure 3. Force versus displacement for the standard (continuous) and truncated (point–dash) methods for case 2

The pseudodynamic method is usually a rather slow process that may take hours to simulate events that represent only seconds, so, if a pseudodynamic test can be made to last an hour rather than four say, it is already a bonus. Another aspect of importance is that the pseudodynamic scheme can be run much like any other finite element scheme, for example: sub-structuring methods can be used to append higher-order systems, however, this tends to broaden the spectral response of the system. Because of the time-step limitations of the central difference scheme this would imply using a very small time step.

In the example presented below none of these severe conditions were prevalent. It was intended to show that the modal truncation method works well with a large experimental system. Also, the system tested contains a highly non-linear element; namely, the isolators made from rubber bearings.

The input force was a scaled version of the Kalamata earthquake of 1987. The following stiffness (measured directly from the test specimen) and mass matrices (imposed) result in the eigenmodes and eigenvalues given below:

$$\mathbf{K} = \begin{pmatrix} 6{\cdot}97668\mathrm{e}+6 & -78{\cdot}7644\mathrm{e}+6 & 23{\cdot}785080\mathrm{e}+6 & -3{\cdot}28344\mathrm{e}+6 \\ -66{\cdot}5360\mathrm{e}+6 & 149{\cdot}8389\mathrm{e}+6 & -110{\cdot}0886\mathrm{e}+6 & 26{\cdot}4043\mathrm{e}+6 \\ 20{\cdot}2572\mathrm{e}+6 & -110{\cdot}8624\mathrm{e}+6 & 166{\cdot}7318\mathrm{e}+6 & -75{\cdot}4955\mathrm{e}+6 \\ -2{\cdot}8483\mathrm{e}+6 & 26{\cdot}8946\mathrm{e}+6 & -76{\cdot}3403\mathrm{e}+6 & 51{\cdot}9976\mathrm{e}+6 \end{pmatrix}$$

$$\mathbf{M} = \begin{pmatrix} 34\,700 & 0 & 0 & 0 \\ 0 & 34\,700 & 0 & 0 \\ 0 & 0 & 34\,700 & 0 \\ 0 & 0 & 0 & 32\,900 \end{pmatrix}$$

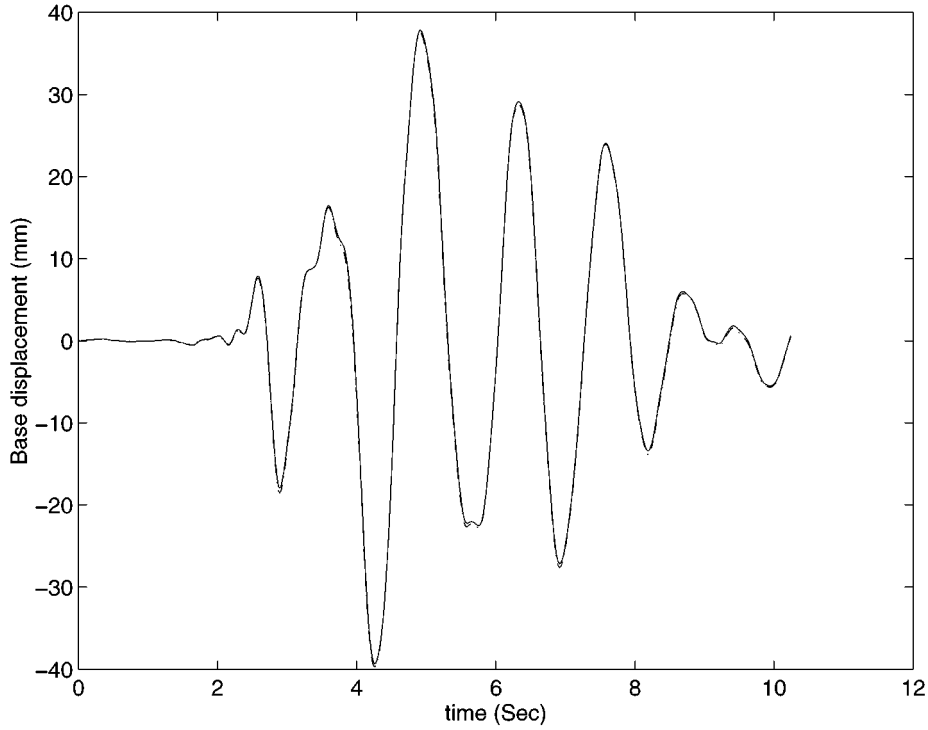

Figure 4. Base displacement of isolated steel frame versus time signals of standard (continuous) and truncated (point–dash) methods, subjected to Kalamata earthquake accelerogramme using pseudo-dynamic test

$$\Psi = \begin{pmatrix} 0{\cdot}22754 & 0{\cdot}6338 & 0{\cdot}6831 & 0{\cdot}3824 \\ -0{\cdot}6245 & -0{\cdot}4400 & 0{\cdot}3832 & 0{\cdot}4668 \\ 0{\cdot}6730 & -0{\cdot}4556 & -0{\cdot}1220 & 0.5371 \\ -0{\cdot}2852 & 0{\cdot}4440 & -0{\cdot}6096 & 0{\cdot}5894 \end{pmatrix}$$

$$\omega = \begin{pmatrix} 94{\cdot}5003 & 0 & 0 & 0 \\ 0 & 55{\cdot}0224 & 0 & 0 \\ 0 & 0 & 26{\cdot}4445 & 0 \\ 0 & 0 & 0 & 7{\cdot}5508 \end{pmatrix}$$

It was decided to eliminate the fourth mode by modal truncation, and, given the reduced number of degrees of freedom, this was done by setting $\gamma_4 = 0$ in the form of expression (40).

Figure 4 shows the displacement at the base of the structure (this position is coincident with the position of the rubber bearings) obtained with the standard and truncated central difference algorithms. The truncated and standard forms follow each other rather well. The comparison is best described qualitatively by Figure 5, which shows the hysteresis loops for the total shear force versus base displacement. The slight differences are probably due to the path dependency of the rubber bearings (in the sense of testing and retesting them) rather than any truncation effects. The method is therefore seen to perform well for a generic, inelastic, structural system.

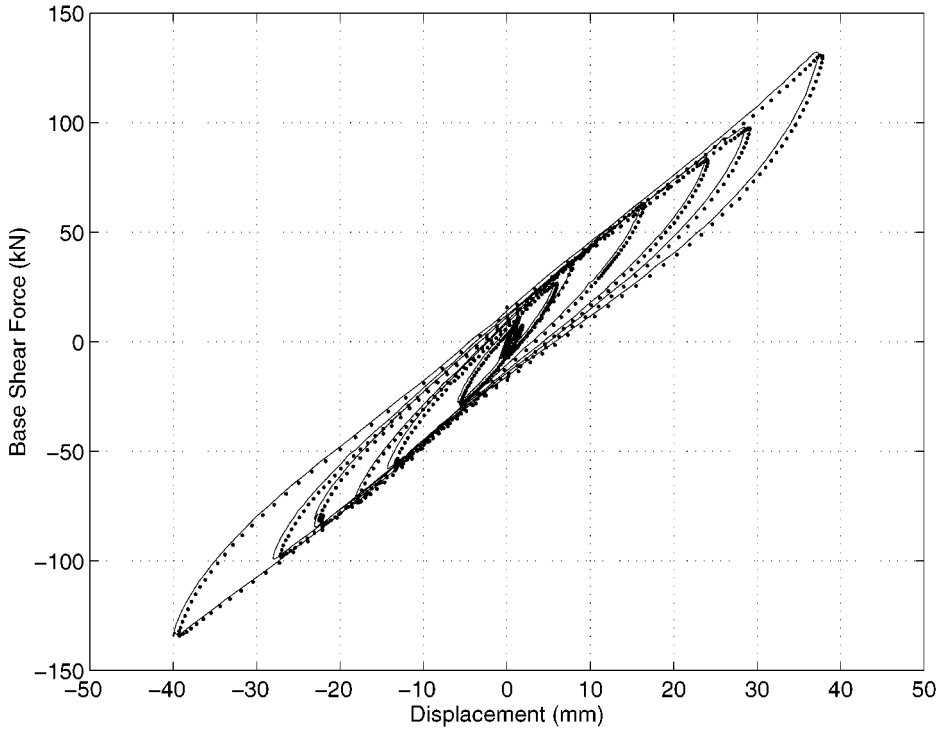

Figure 5. Total base shear load versus base displacement hysteresis loops of isolated structure, using standard (continuous) and truncated (point–dash) methods

The results may also be represented in the spectral domain as shown in Figure 6. In this figure the spectral content of the forces, measured at the second-storey level, reveal that only three peaks appear when the truncated central difference algorithm is used, whereas all four components appear in the standard case.

6. COMMENTS ON THE APPLICABILITY OF MODAL TRUNCATION

The applicability of the modal truncation method described above is subject to engineering judgement. In some cases, particularly if one is using a very large time step, some errors may occur as a consequence of sudden stiffness changes or unloading sequences during a time step. This is independent of the convergence criteria established in Section 4. The error is generated when the stiffness matrix of the previous time step is extrapolated onto the new displacement field where it may no longer be consistent with the system state variables. Stability criteria are a necessary condition in order to perform numerical integration, however for hysteretic systems, accuracy is determined by the time step. Thus, if the time step is too large, certain stiffness transitions will not be resolved accurately; in spite of this the numerical procedure remains stable.

It is implied that the time step chosen for the truncated mode set, although relatively larger and hence cheaper than the standard, should still be small enough to provide sufficient accuracy to capture the transition points associated with stiffness and unloading discontinuities. For systems that have relatively narrow bandwidths the use of a large time step used in conjunction with modal truncation may be too severe and errors may be generated. It is clear that at some stage there would be no benefit in resorting to using a bigger time step if the accuracy was poor. However, in those cases where such errors may arise, a large time

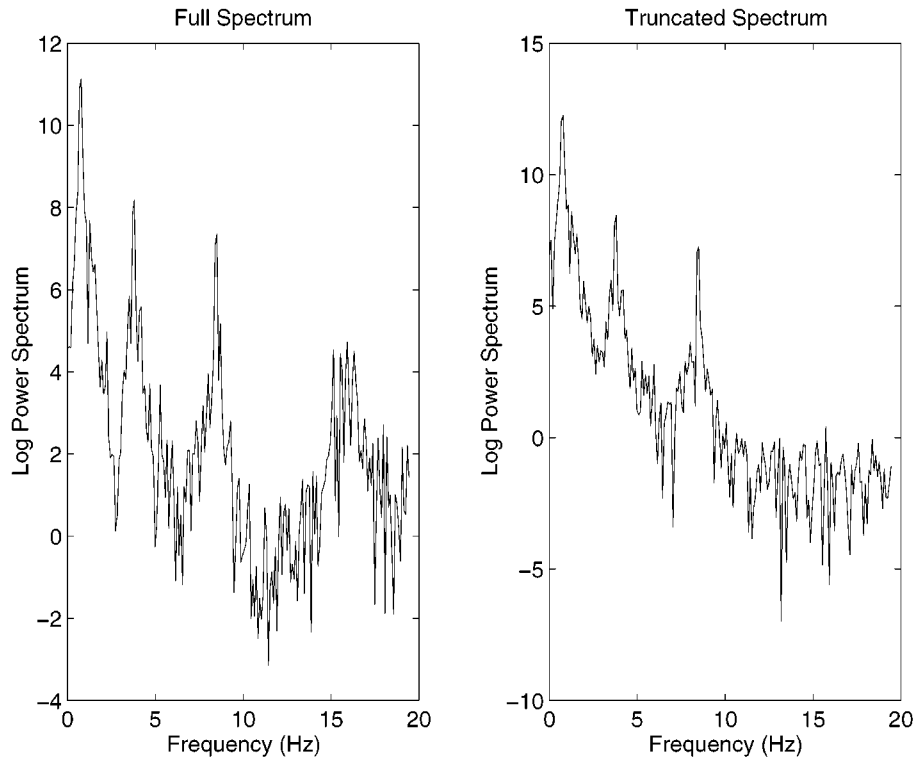

Figure 6. Spectral content of second storey force signals obtained from pseudodynamic tests using standard and truncated methods

step could be used if it were possible to use the modal truncation in conjunction with interpolation procedures, such as that suggested by Chen and Robinson,[15] that trace the time at which the structural change occurs. The technique can be used to predict the intermediate time by adjusting the differential equations via a change of variable that result in two coupled differential equations.

To close we would like to make the following qualification. The scope of this truncation method is to improve the stability of explicit numerical schemes so that they can be used economically in very large (or widely varying eigenvalue) systems. In this sense it must be understood that when there is a very large difference in the ratio of the sufficient time step (in the sense of accuracy) as opposed to the necessary time step (in the sense of numerical stability), then it would be convenient to use modal truncation directly.

Another aspect concerns the suitability of this method for systems that are dominated by intermediate frequencies. The problem for these lies not so much in solving the associated eigenproblem (this need only be performed when the structural dynamics problem is configured), rather, we must consider the ratio between the time constants of the intermediate modes and that demanded by stability for the highest modes. Once again, the user must decide when considerations of accuracy impinge on numerical efficiency and stability.

We presume that the mathematical proof based on modal decomposition will validate the applicability to systems having many thousands of degrees of freedom. The next stage in the investigation is to apply the truncation method on very large systems where we would hope to see the benefits in terms of reduced costs. One interesting and curious application is being prepared in the field of molecular dynamics. Molecules are usually modelled as structural systems—of a sort—characterized by various interaction forces. These forces have their origin in the attracting–repelling potential wells: some, Van der Waals for example, are far-field (low frequency) whereas the inter-atomic forces are of much higher-frequency content. The numerical

problem when modelling molecular systems arises when dynamic events associated to the long-term behaviour of molecules (such as protein folding) are conditioned by the very high frequencies associated with inter-atomic vibrations.

7. CONCLUSIONS

A formulation has been presented with which it is possible to express numerical integration algorithms for structural dynamics in a hybrid Cartesian-spectral basis. The method consists in subtracting the projection, onto Cartesian co-ordinates, of a reduced invariant spectral set. The invariant set is usually linked to high-frequency modes which are artificially generated from fine mesh geometry, but which do not contribute substantially to the observed dynamic response. The number of the original Cartesian co-ordinates used in the proposed method is preserved, however, the size of the original spectral basis that spanned the Cartesian set is attenuated or reduced. The formulation remains explicit. No basis changes are implemented during the numerical integration computations: the truncated basis is chosen at the outset from the reduced eigenvalue problem and is kept constant. The numerical analysis suggests that, for the untruncated modes, the formulation is second-order accurate. The method has been applied successfully to non-linear MDoF systems, one being purely numerical, the other experimentally on the pseudodynamic test method.

APPENDIX

Notation

$\mathbf{M}$	mass matrix
$\mathbf{K}$	stiffness matrix
T'	period distortion
$\mathbf{X}$	displacement vector
$\mathbf{X}^n$	time-discretized form of $\mathbf{X}$
x	modal displacement co-ordinate
x^n	time-discretized form of x
β, γ	weighting parameters
ω	natural frequency
λ	eigenvalue
$\bar{\zeta}$	equivalent numerical damping
$\mathbf{\Psi}$	matrix of orthonormalized eigenvector
Δt	time increment
$\omega\Delta t$	sampling frequency
$\bar{\Omega}$	effective sampling frequency

ACKNOWLEDGEMENTS

The authors would like to acknowledge the collaboration of G. Magonette in conducting the pseudodynamic tests.

REFERENCES

1. J. Chung and G. M. Hulbert, 'A time integration algorithm for structural dynamics with improved numerical dissipation: the generalised- method', *Trans. ASME, J. Appl. Mech.* **60**, 371–375 (1993).
2. H. M. Hilber, T. J. R. Hughes and R. L. Taylor, 'Improved numerical dissipation for the time integration algorithms in structural dynamics', *Earthquake Engrg. Struct. Dyn.* **5**, 283–292 (1977).

3. T. J. R. Hughes and W. K. Liu, 'Implicit–explicit finite elements in transient analysis: stability theory', *Trans. ASME, J. Appl. Mech.* **45**, 371–374 (1978).
4. T. Belytschko and R. Mullen, 'Stability of explicit-implicit mesh partitions in time integration', *Int. J. Numer. Meth. Engrg.* **12**, 1575–1586 (1978).
5. M. Nakashima, T. Kaminosono, M. Ishida and K. Ando, 'Integration techniques for substructure pseudo dynamic test', *Proc. 4th U.S. Nat. Conf. on Earthquake Engrg.* vol. 2, (1990), pp. 515–524.
6. S. R. Idelsohn and A. Cardona, 'Reduction methods and explicit time integration technique in structural dynamics', *Adv. Engng. Software* **6**, 36–44 (1984).
7. B. Mohraz, F. E. Elghadamasi, and C. J. Chang, 'An incremental mode-superposition for non-linear dynamic analysis', *Earthquake Engrg. Struct. Dyn.* **20**, 471–481 (1991).
8. P. Leger and S. Dussault, 'Non-linear seismic response analysis using vector superposition methods', *Earthquake Engrg. Struct. Dyn.* **21**, 163–176 (1992).
9. K. J. Bathe, *Finite Element Procedures in Engineering Analysis*, Prentice-Hall, Inc., Englewood cliffs, NJ, 1982.
10. T. J. R. Hughes, *The Finite Element Method*, Prentice-Hall, Englewood Cliffs, NJ, 1987.
11. S. Shing and A. Mahin, 'Computational aspects of a seismic performance test method using on-line computer control', *Earthquake Engrg. Struct. Dyn.* **13**, 507–526 (1985).
12. R. W. Clough, 'Effect of stiffness degradation on earthquake ductility requirements', *Structures Materials Report No.* 66-16, Dept. of Civil Engineering, Univ. of Calif., Berkeley, CA, 1966.
13. E. Gutiérrez, G. Magonette, J. Molina, D. Tirelli and G. Verzeletti, 'Methodology for the vibration-isolation testing of full-scale structures fitted with rate dependent rubber bearings' *Proc. 1st European Conf. On Struc. Control,* World Scientific, Singapore, 1996, pp. 306–313.
14. C. R. Thewalt and S. A. Mahin, *Hybrid Solution Techniques for Generalised Pseudodynamic Testing Report No. UCB/EERC-87/09,* University of California Berkeley, July 1987.
15. C. C Chen and A. R. Robinson, 'Improved time-history analysis for structural dynamics. I: treatment of rapid variation of excitation and material non-linearity', *J. Engrg. Mech.* **119** (12), 2496–2513 (1993).

